https://doi.org/10.5194/egusphere-2026-1818
Preprint. Discussion started: 10 April 2026

Microbial carbon use efficiency emerges from interactions between soil structure and life-history strategies

Maëlle Maestrali[1], Naoise Nunan[1], Antsa Sarobidy-Randrianantenaina[1], Haotian Wu[2], Steffen A. Schweizer[2], Xavier Raynaud[1]

1Sorbonne Université, Université Paris Cité, Univ Paris Est Créteil, CNRS, IRD, INRAE, Institut d'écologie et des sciences de l'environnement de Paris, IEES, F-75005 Paris, France

2 Technical University of Munich, TUM, School of Life Science, Chair of Soil Science, Emil-Ramann Strasse 2, 85354, Freising, Germany

Correspondence to: Maëlle Maestrali (maelle.maestrali@sorbonne-universite.fr)

Abstract

Microbial carbon use efficiency (CUE) is believed to be a key regulator of the accumulation of persistent soil organic carbon. Microbial processing of organic carbon in soil occurs in the pore network, the properties of which are known to affect microbial activity. However, the effects of interactions between pore architecture, and microbial life-history strategies on carbon dynamics, and house these interactions are modulated by moisture regime, remain poorly understood.

Here, we use a spatially explicit model based on a cellular automaton, applied to realistic soil pore networks derived from X-ray tomographic images, to investigate how pore geometry and organic matter distribution shape microbial dynamics and CUE. The model explicitly represents r- and K-strategists that are either motile or immobile, and have different resource requirements for growth, maintenance and motility. The constraints imposed on substrate diffusion and the spatial domain in which motile bacteria can effectively disperse by the moisture regime are explicitly represented in the model, in order to capture how moisture regulate decomposer access to resources.

The simulations show that pore architecture has a significant effect on microbial CUE. Micropores promoted high CUE and a dominance of K-strategists by limiting substrate diffusion, reducing pore connectivity, and constraining microbial access to spatially isolated resources. In contrast, macropores with high connectivity and greater substrate accessibility favor r-strategists, rapid biomass turnover and lower CUE. Motility emerges as advantageous in connected, carbon-rich macropores, but energetically unfavourable in confined or poorly connected micropores, where immobile strategies outperform motile ones.

Overall, our results indicate that microbial CUE is not an intrinsic property of life-strategies alone, but emerges from the interaction between microbial life-strategies and pore-scale physical constraints. This study suggests that soil structure influences microbial strategies by limiting resource availability and dispersal.

Introduction

Soil structure refers to the three-dimensional spatial arrangement of solid constituents and voids at different scales (Rabot et al., 2018). Soil pore space is directly linked to soil functions because it governs air/water transport and microbial colonization (Kravchenko et al., 2020; Schlüter et al., 2020). which are essential for determining the efficiency of microbial processes and the carbon cycle (Kravchenko and Guber, 2017; Schimel and Schaeffer, 2012). The size and connectivity of soil pores regulate nutrient diffusion and gas exchange, which can

https://doi.org/10.5194/egusphere-2026-1818
Preprint. Discussion started: 10 April 2026

profoundly affect the survival and colonization of microenvironments by microorganisms (Kravchenko and Guber, 2017; Schlüter et al., 2022). In soil, microorganisms tend to selectively inhabit soil pores of different sizes (Li et al., 2024). It has been suggested that the properties of the pores in which microbial decomposers are active influence the rates of OM decomposition and, thus, its persistence (Kravchenko and Guber, 2017; Chenu et al., 2025); Maestrali et al., 2026). The fate of organic carbon (OC) depends largely on the capactity of the microorganisms present to use the OC and the spatial access the have the OC (Lehmann et al., 2020; Shi et al., 2021). The decomposition of OC depends on the encounter between organic matter (OM) and decomposers or their decomposing enzymes. If this encounter is limited by the structural properties of the microbial environment, decomposition cannot take place, regardless of the properties of the OM (Dignac et al., 2017).

While pores with throat diameters < 1 µm are generally inaccessible to microbes, due to size exclusion, pores between 1 and 10 µm can be colonized by microorganisms, depending on their connectivity to the surrounding pore network. Larger pores (> 10 µm) offer more space for microbial colonies and fungal hyphae. Previous studies suggest that pore size and connectivity influence the distribution of microbial strategies, with fast-growing copiotrophs often associated with well-connected, resource-rich environments, and slow-growing oligotrophs dominating in more isolated or resource-limited conditions (Li et al., 2024). However, the extent to which interactions among the physical structure of the pore network, the spatial distribution of resources and the life-cycle strategies of microorganisms regulate microbial activity and carbon use efficiency is poorly understood. There is still a lack of mechanistic and spatially explicit understanding of how pore size, resource distribution, and microbial life-history strategies jointly regulate microbial processing of resources and the resulting carbon dynamics.

The different micorenvironments that occur in the pore network have been classified into according to, among others, resource availability (Li et al., 2024). The differences in conditions, naturally, exert selective pressures on the microbial communities which are more adapted to high or low levels of resource availability. The r/K selection theory provides a simple and widely used framework for interpreting the dynamics and distribution of soil microorganisms (Fierer et al., 2007; Peng et al., 2022). While the r- and K-selection framework does not capture the full complexity of microbial life-history strategies (Reznick et al., 2002), it provides a simple and intuitive way to represent key ecological trade-offs. According to this classification scheme, r-strategists favour resource-rich conditions (copiotrophic species) but perform poorly when nutrient availability is low, while K-strategists grow more slowly but perform relatively better in resource-poor environments (oligotrophic species) (Fierer et al., 2007; Gao et al., 2025; Zheng et al., 2024). Therefore, the r/K selection theory is likely appropriate for this kind of system.

Motility is another trait that allows microorganisms to adapt to their microenvironment: the ability to move in the porous soil environment can confer a selective advantage under certain conditions. Although direct observations of microbial motility in unsaturated soils remain technically challenging due to the opacity and complexity of soil (Wang and Or, 2010), several studies indicate that soil moisture and pore network structure control microbial motility by regulating water film continuity and spatial connectivity within the pore space (Barton, 1997; Chang et al., 2009; Or et al., 2007; Young and Crawford, 2004). In particular, the presence of continuous water films is necessary for flagellar motility, which limits its expression in dry soils. As motility is energetically cost-

https://doi.org/10.5194/egusphere-2026-1818
Preprint. Discussion started: 10 April 2026

ly, its prevalence also appears to be modulated by the availability of organic carbon, an essential resource for microbial metabolism. Thus, carbon-rich environments, such as rhizospheres, tend to favour motile bacteria, as evidenced by higher levels of flagellar genes detected in these areas (Ramoneda et al., 2024). Conversely, in more resource-poor or arid environments, motility is often less prevalent. However, the role of pore-scale geometry particularly pore size distribution and connectivity in modulating the costs and benefits of motility remains poorly quantified. In particular, it is still unclear how physical constraints and spatial resource heterogeneity interact to determine when motility enhances microbial growth and carbon use efficiency.

The modelling of soil processes has made great strides due to the development of spatially explicit, mechanistic approaches that account for the physical structure of soil (Ray et al., 2017; Ritschel and Totsche, 2019; Rötzer et al., 2025; Zech et al., 2022). However, these models focus primarily on physical heterogeneity and do not always account for the functional diversity of microbial communities. The integration of realistic soil structure with explicit microbial ecological dynamics remains a major challenge (Baveye et al., 2011; Otten et al., 2001; Pot et al., 2021). With some notable exceptions (Allison, 2005) approaches tend to separate these aspects: models focused on microbial processes often consider homogeneous environments, while models that account for soil heterogeneity generally ignore microbial traits and interactions (Panikov, 1999). This disconnection impairs our understanding of the mechanisms underlying microbial carbon use in structured environments. Here, we use a cellular automaton framework which explicitly represents spatial structure and microbial interactions that are based on local rules, in order to determine how microbial traits affect C processing under different local environmental conditions.

The framework includes distinctive physiological traits for r- and K-strategists, different types of motility, resource distributions and moisture regimes. The spatial structure of the environment was derived from X-ray tomographic images of soil. .

Material and methods

2.1 General principles of the cellular automaton

A cellular automaton is a discrete mathematical model composed of a regular grid of cells, each of which can adopt a finite number of states. The system evolves over time in synchronous steps, where the future state of each cell is determined by its current state and that of its neighboring cells, according to a set of predefined transition rules (Wolfram, 2002). In the context of this study, each cell represents a microscopic spatial unit in which explicit spatial interactions among microbial cells, as well as between microbial cells and organic substrates, can occur. The system is based on two coupled matrices of 100 × 100 cells (pixels).

The state matrix, which identifies the nature of each grid cell in the automaton. Eight distinct cellular states are included, corresponding to different soil components or biological types: (1) solid phase of the soil, (2) air-filled porosity, (3) water-filled porosity, (4) carbon resources, (5) motile r-strategists, (6) immobile r-strategists, (7) motile K-strategists, and (8) immobile K-strategists (Table S1).

https://doi.org/10.5194/egusphere-2026-1818
Preprint. Discussion started: 10 April 2026

The resource matrix, which quantifies the amount of resources associated with each grid cell (when applicable). This matrix is used to monitor carbon flows in the system. This dual architecture makes it possible to model the system's structure and resources separately.

2.2 Construction of the state matrix

X-ray micro-tomographic images of a Luvisol (resolution 19 µm), obtained from the Soil Structure Library (https://structurelib.ufz.de/lit/) in the form of a TIFF image stack, were used to create the state matrix.

2.2.1 Soil images

Ten regions (100×100 pixels) were randomly selected from different images of the image stacks. If a region did not contain any usable pores (i.e., no empty space or, conversely, no solid matter), it was discarded and another one was extracted. The 10 image regions were thresholded using the Otsu method to separate pores and solid phases (Smet et al., 2018).

2.2.2 Optimization of pore connectivity

Since image resolution tends to obscure the narrower pores and reduce the connectivity of the porous network, we applied Bresenham's algorithm to the 10 thresholded images in order to establish connections between physically close but unconnected pores (Bresenham, 1965). This method establishes connections based on the relative distance, spatial orientation, and surrounding configuration of the pores (Bresenham, 1965).

2.2.3 Pore classification and characterization

The classification and characterization of pores in the thresholded images consisted of a sequence of steps that began with a morphological erosion to extract the skeleton of the pore network. The pores were then classified based on the distance between each pixel of the skeleton and the nearest solid phase pixel. Pores for which the skeleton pixels were at a distance of less than 4 pixels (4µm) were considered micropores (small, S). Other pores were classified as macropores (large, L). The images contained on average 22.89 ± 2.13% macroporosity and 17.09 ± 1.61% microporosity.

2.2.4 Distribution of resources within the pore network

Resources were placed either in small or in large pores (Fig. 1). The resources were distributed so that the concentration of resources in each pore size class was the same. The resources occupied 2.83% of the surface area of the 2D matrix, which is less than what is generally found in soil (5-25% soil volume, refs). However, all the resources were placed in the pore network and were therefore readily available to microbial decomposers, which is not the case in soil. Generally, <20% is readily available in soil (Bongiorno et al., 2019; Haynes, 2005; McLauchlan and Hobbie, 2004). The amount of resources added therefore approximated the amount of readily available resources found in soils. For this study, each resource cell contained 100 resource units, but additional simulations examined the effect of varying the concentration of resource cells (Fig. S8)

https://doi.org/10.5194/egusphere-2026-1818
Preprint. Discussion started: 10 April 2026

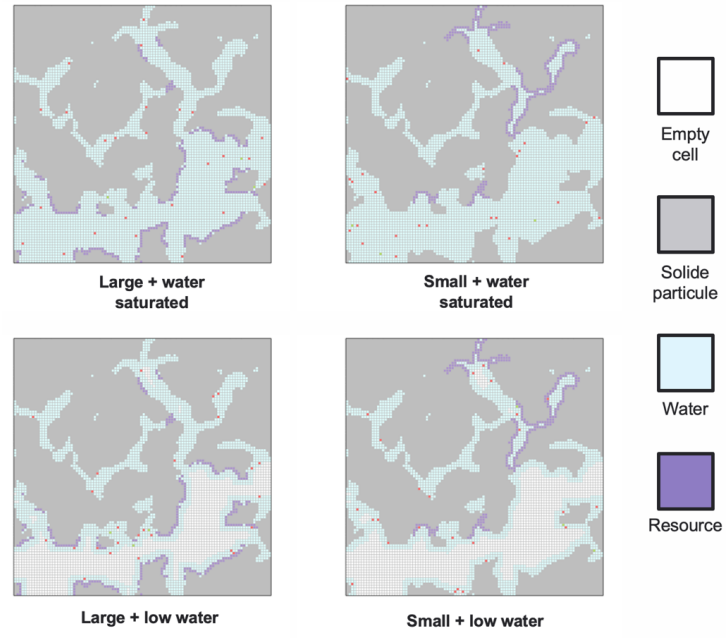

Figure 1 : Diagram showing the four initial conditions of moisture and resource distribution for a given matrix. The isolated green and red pixels that are barely visible on the grids represent microbial cells randomly placed at the start of each simulation.

2.2.3 Moisture management in matrices

Each matrix was assigned a specific moisture level. Moisture was distributed throughout the pore space by adding a layer of water pixels next to the solid surface. Further layers of moisture pixels were then added in succession until the desired moisture level was reached. This process is akin to morphological dilation and results in the narrower pores being filled first. In addition, dilation ensures the connectivity of the pore network from the start of the simulations without creating heterogeneity between large and small pores (Fig. 1).

2.3 General automaton rules

The cellular automaton model used here is based on a set of deterministic rules applied synchronously at each simulation time step, modifying both the state matrix and the resource matrix. In each matrix, only water-filled pore grid units, resources grid units and microbial cells can change state. Within a simulation, solid phase grid units and empty pores are immutable and represent the inherent constraints of a particular matrix (Fig. 2).

The resource base of the system is defined at the start of the simulation in the form of resource elements, 100 of which is assigned to each resource grid unit. The resource can diffuse from its initial locations in the matrix according to a propagation model that follows Moore's neighbourhood (eight adjacent grid unit) (Zaitsev, 2017). This diffusion occurs along concentration gradients, with resource spreading from resource-rich to resource-poor zones. Mathematically, the change in the resource content of a resource grid unit at coordinates (x,y) is described by the equation Resource x,y(i+1) = Resource x,y(i) - Σ Resource (i), where i represents the current iteration. At each iteration, only cells whose resource content exceeds a minimum threshold (diffusion threshold) can act as

https://doi.org/10.5194/egusphere-2026-1818
Preprint. Discussion started: 10 April 2026

donors, preventing very small resource quantities from spreading. The amount of resource transferred to each eligible neighbor is not proportional to the concentration gradient but is instead capped by a fixed maximum value (diffusion rate). As a result, resource-rich cells lose a constant quantity of resource to each less concentrated neighboring cell, leading to a stepwise and locally asymmetric redistribution process. This mechanism produces a gradual homogenization of resource distribution across the matrix without reaching instantaneous equilibrium.

The different types of microbial cells (Table 1) transition between three states (growth, maintenance or death), depending on resource availability. The transitions are regulated by three critical resource thresholds. The maintenance threshold (Sd) triggers a state of reduced metabolism when resources become scarce. During maintenance, cells do not move or reproduce. If the resource scarcity persists and falls below the mortality threshold (Sm < Sd), the microbial cell dies and the remaining resource is transferred to the available resource pool. Conversely, the accumulation of resource above the reproduction threshold (Sr) activates cell division, in which a new cell of the same type appears in any of the eight adjacent aqueous grid units. The parent cell invests a significant proportion of its resource (25 to 50% depending on the microbial strategy) in this process according to the formula Resource (parent, t+1) =Resource (parent, t) - [Resource(descendant) + Cr], where Cr represents the fixed metabolic cost of reproduction (Table 1). The reproductive costs vary among microbial cell types, the cost being higher for K-strategists.

Motile cells can search for and exploit available resources within a configurable perception radius R. Motile cells move at a speed of one grid unit per iteration towards the nearest and most resource-concentrated resource grid unit within their perception radius. Due to the cost of motility, motile cells focus only on resources with a resource content above a defined threshold equal to 5 resource elements (Table 1). The cost of motility (Cm) is deducted for each move according to Resource (t+1) = Resource(t) - Cm. The inability of mobile cells to anticipate obstacles, such as pore walls, when moving toward the nearest resources introduces a realistic constraint that limits their effectiveness in complex environments. Immobile cells rely entirely on the diffusion of resources to acquire the resource and matter necessary for maintenance and growth. This resource acquisition strategy is energetically more economical, due to the absence of motility costs.

https://doi.org/10.5194/egusphere-2026-1818
Preprint. Discussion started: 10 April 2026

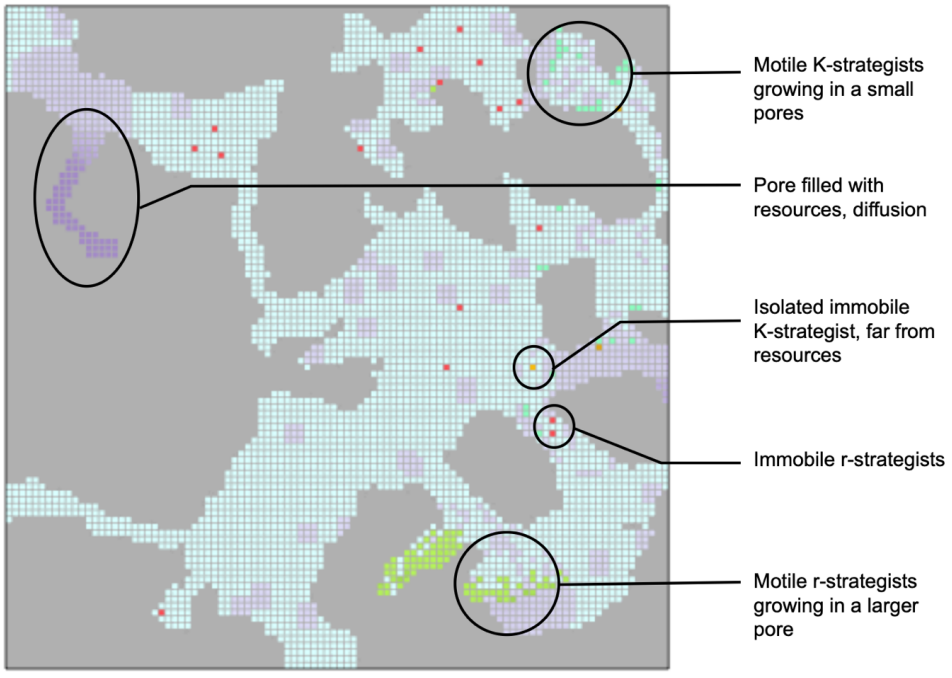

Figure 2 : Image taken from one of the simulations showing strategists r and K present simultaneously in the matrix (iteration 50). The different colors represent the various states of the cells: light blue for water, gray for the solid phase of the soil, purple for resources (with the intensity of the purple indicating the concentration of resources), green for mobile cells, and red/orange for immobile cells.

Table 1 : Different cell types present in the simulations, and the associated resource costs and thresholds

Cell type	Motility	Motility cost	Maintenance cost	Dormancy threshold	Mortality threshold	Reproduction cost (Cr)	Reproduction threshold
r-strategist cells	Mobile	1	1	60	30	55	100
	Immobile	0	1	60	30	55	100
K-strategist cells	Mobile	5	3	60	30	70	250
	Immobile	0	3	60	30	70	250

2.3 Simulation runs

Four initial matrices were generated for each of the 10 images previously extracted. Each initial matrix was generated with a combination of different moisture levels (saturation or low water) and resource distributions (resources were placed in either large pores or small pores). During the simulations, different microbial densities (low 23 bacterias, and high 56 bacterias) and microbial diversities (r, K and r+K) were applied (Fig. 2). Twenty simulations of 200 iterations were then run on each matrix, resulting in a total of 400 simulations.

https://doi.org/10.5194/egusphere-2026-1818
Preprint. Discussion started: 10 April 2026

2.4 Sensitivity analysis of the model

In addition to the simulations presented above, analyses were performed to establish the sensitivity of the model to (1) matrix moisture, (2) initial resource concentration, and (3) the parameters governing the r- and K-strategies. Details of the methods and results obtained for these additional simulations are presented in supplementary data.

2.5 Model parametrisation and realism

At the beginning of the simulations, microbial biomass represented between 9.0% (low microbial density) and 16.5% (high microbial density) of total soil organic carbon (SOC). These values were chosen as they are representative of the rhizosphere, a highly active soil compartment characterized by elevated microbial densities relative to total organic carbon (Chunhua Lv, 2022; Zhao et al., 2022). Although microbial biomass is often reported to represent a smaller fraction of SOC in bulk soils, typically reaching up to ~6% in field measurements (He et al., 2021), estimates based on fumigation–incubation methods indicate microbial biomass carbon contents ranging from 300 to 1200 mg C kg^{-1} in natural silt–clay soils (Franzluebbers et al., 1994; Jenkinson and Powlson, 1976; Sparling and West, 1988), corresponding to approximately 1.5–12% of SOC in soils containing 1–2% total organic carbon. The values used in the present model therefore fall within, or slightly above, the upper range reported in the literature, consistent with a focus on the rhizosphere rather than bulk soil. Within the model, the use of relatively high initial microbial densities aimed to ensure the establishment and persistence of microbial populations over the simulation period, while allowing a representative distribution of different functional types across heterogeneous microenvironments (pores of varying size and resource availability). Although the model assumes an identical total amount of carbon between pore types, the differential accessibility generated by diffusion constraints and spatial geometry conceptually reproduces empirical gradients. Cells were initially distributed randomly in space to avoid imposing predefined spatial advantages among microbial types (mobile vs. immobile) and life-history strategies (r vs. K), thereby allowing differences in colonization dynamics to emerge from intrinsic traits and interactions.

In the model, the recycling rate of microbial biomass (cellular resource resource) was set to 100%, meaning that the entire resource content of dead cells was instantaneously transferred to the pool of assimilable resources. This assumption implies an immediate decomposition of cellular structures and the absence of a non-assimilable organic matter compartment. Empirical studies indicate that microbial biomass recycling efficiency in soils is much lower. Although microbes are able to feed on microbial necromass, recycling efficiencies rarely exceed 12% (Kästner et al., 2021), and microbial necromass can constitute more than half of total soil organic carbon stocks (Liang et al., 2019). The use of a 100% recycling rate therefore does not aim to represent realistic microbial necromass processing, but rather reflects a deliberate structural simplification of the model. All cellular resource is assumed to be potentially accessible to other microbes, corresponding to an idealized and instantaneous transformation of biomass into assimilable resources. As a consequence, the model accelerates carbon transformation processes compared to real soil systems and likely overestimates the efficiency and speed of microbial biomass recycling. This limitation should be kept in mind when interpreting model outcomes.

https://doi.org/10.5194/egusphere-2026-1818
Preprint. Discussion started: 10 April 2026

2.6 Statistical analysis

All statistical analyses were performed using R (R: The R Project for Statistical Computing, 2026). The demography of microbial populations, their use of resources for maintenance, growth and movement, and the temporal dynamics of resources were monitored for each simulation. Microbial carbon use efficiency (CUE) was calculated according to the formula: CUE = Resources assimilated (t) / Resources consumed, with resources consumed = resources assimilated into biomass + resources released through breathing. This ratio made it possible to assess the influence of multiple factors on the metabolic efficiency of microbial communities: resource location, water regime, adaptive strategies and microbial motility. The CUE was calculated for the entire community of cells present in the matrix at each iteration, and then an average CUE for each simulation was also calculated from the 25th iteration to the end of the simulation, to avoid taking into account the cell installation time during the first iterations, during which the CUE values were highly unstable.

Results

3.1 Populations dynamics

The population dynamics profiles of r- and K-strategists (Fig. 3) were similar regardless of the number of microbial cells initially present in the simulation (28 or 56). The mortality of immobile K-strategists was very high during the first 50 iterations (Fig. 3a) and was directly linked to their initial position in the matrix: if they were positioned too far from resources, the diffusion rates of resources were not sufficiently high to satisfy their energetic requirements for survival. Compared to immobile K-strategists, immobile r-strategists (Fig. 3b) reproduced more easily, due to their lower reproduction threshold. As a result, a small population peak was observed between iterations 50 and 80 (Fig. 3b). Thereafter, resource limitation caused a decrease in population size as cell death rates surpassed reproduction rates. It is interesting to note that the largest immobile populations were found in the large pores. However, immobile populations persisted longer in small pores, especially at low moisture levels. The most unfavourable initial configuration for the persistence of immobile populations over time was when resources were in large, water-saturated pores.

https://doi.org/10.5194/egusphere-2026-1818
Preprint. Discussion started: 10 April 2026

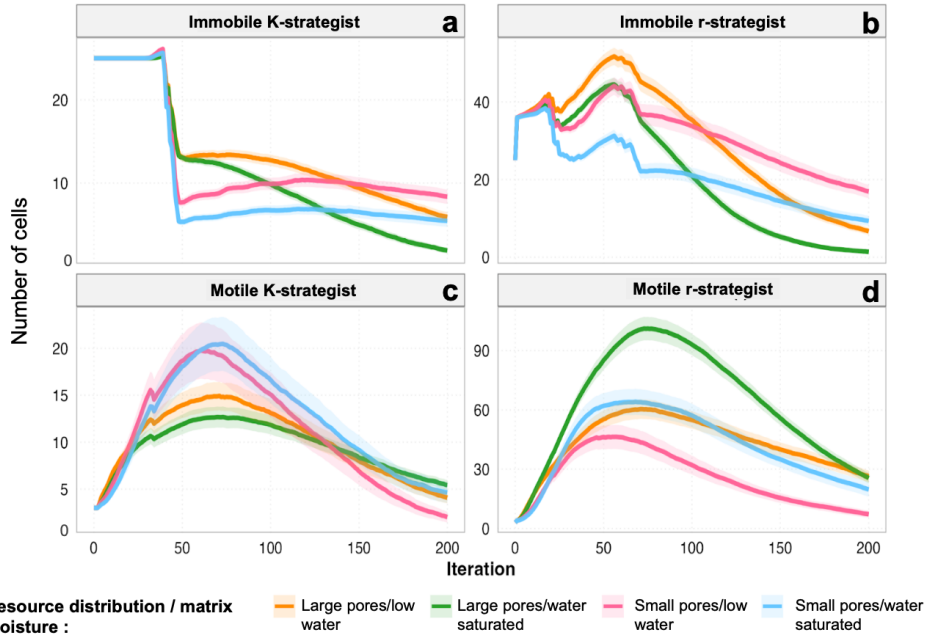

Figure 3 : Number of motile and immobile cells with either r- or K-strategies in simulations with an initial population size of 56 cells (50 immobile and 6 motile). The results of simulations with initial populations of 28 initial cells were similar and are available in the supplementary data (Figure S1). The colours refer to the different initial matrix configurations, where, resources were distributed in the large pores (orange and green) or in the small pores (pink and blue). Matrices were either saturated with water (green and blue) or low water (pink and orange). Note that the y-axis scales are different.

The population dynamics of the motile populations showed an initial increase in size during the first 50 iterations (Fig. 3), which was followed by a decrease, as the populations became resource limited. The results observed for motile populations differed according to the life strategy: the population of r-strategists increased to over 100 cells/matrix while the populations of K-strategists remained more modest at fewer than 40 cells/matrix (Fig. 3c). The populations of K-strategists reached a maximum when the resources were located in small pores, whereas r-strategist populations thrived when resources were in large, water-saturated pores. Neither r- nor K- strategists thrived in the other's preferred environments. The least favourable situation for motile r-strategists was when resources were in small pores with low water content. In this scenario, the environment impeded motility, thus reducing both the rate at which resources were acquired and the reproduction rate.

https://doi.org/10.5194/egusphere-2026-1818
Preprint. Discussion started: 10 April 2026

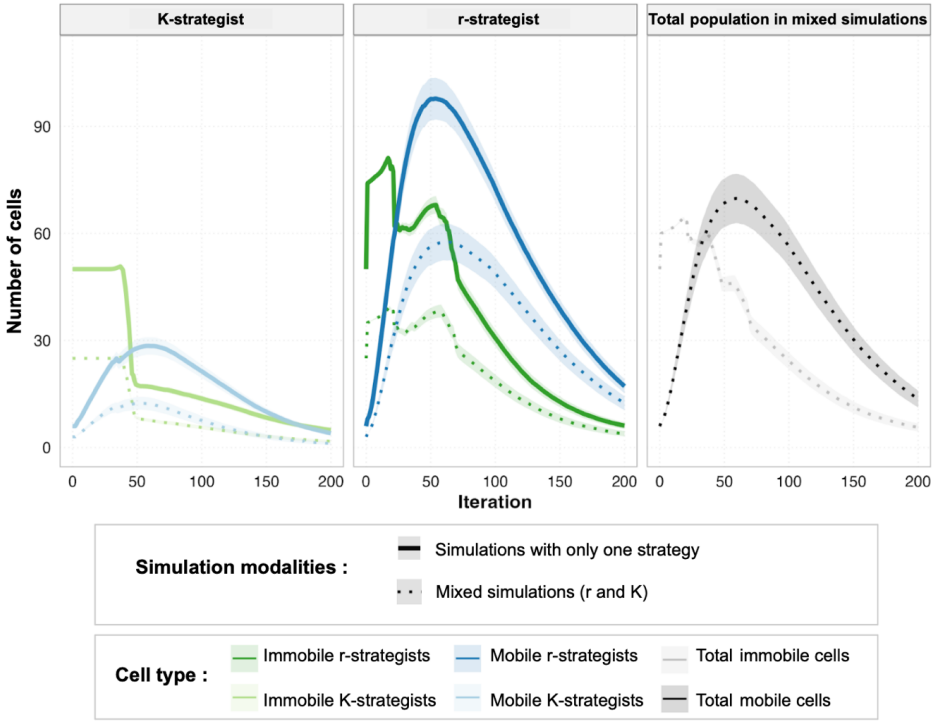

Figure 4: Simulations showing the effects of competition between r- and K-strategists. K-strategists, r-strategists and total cell populations in which r-strategists (28 cells) and K-strategists (28) were present together in the same matrix. The solid lines show simulations without competition which correspond to situations with K strategists only (25 immobile and 3 motile) and r strategists only (25 motile and 3 immobile) respectively. The dashed lines show the results of simulations with competition, where r- and K-strategists were both present in the matrices. The grey curve in the third panel is the sum of the immobile K and r cells in the previous two panels. The black curve on the third panel is the sum of moving K and r strategists on the previous two facets.

Simulations in which both r- and K-strategists were present together showed that competition affected both populations, whether they were motile or immobile, from approximately the 40th iteration onwards, resulting in decreases in population size (Fig.4). This was due to resources becoming more limited relative to the needs of the populations. The competitive interactions resulted in r-strategists dominating the matrix. The same general dynamics can be observed with a larger initial cell supply (56 r-strategists and 56 K-strategists) (Fig.S2).

3.2 Microbial carbon use efficiency

The CUE differed markedly among microbial strategies and initial community sizes (Fig.5). Overall, communities dominated by K-strategists exhibited higher CUE than either those dominated by r-strategists or mixed communities. The highest CUE values were observed in K-strategist communities with low initial cell densities. In contrast, r-strategist communities consistently showed a lower CUE under comparable conditions (Tukey: P<0.001).

https://doi.org/10.5194/egusphere-2026-1818
Preprint. Discussion started: 10 April 2026

Increasing the initial number of cells led to a decrease in CUE for both r- and K-strategist communities, indicating a negative effect of initial density on carbon use efficiency. Mixed communities composed of both r- and K-strategists exhibited the lowest CUE values across all scenarios. Statistical support for these effects is provided in Fig. S3.

In addition to the effects of metabolic strategy and the initial cell numbers, the location of resources in specific pores also had significant effects (F=101.53; P<0.001), as did microbial cell motility (F=138.89; P<0.001) and their interaction (F=328.03; P<0.001).

Firstly, higher CUE values (0.40±0.04 for K cells and 0.39±0.04 for r cells) were always obtained for immobile cells under low water conditions. The next highest, but significantly lower (Tukey: P<0.001), CUE values were obtained when resources were in water saturated small pores (0.36±0.07 for K cells and 0.35±0.04 for r cells). When the resources were in large pores, immobile cells showed the lowest CUE, in particular under water-saturated conditions (0.24±0.04 for K cells and 0.23±0.02 for r cells).

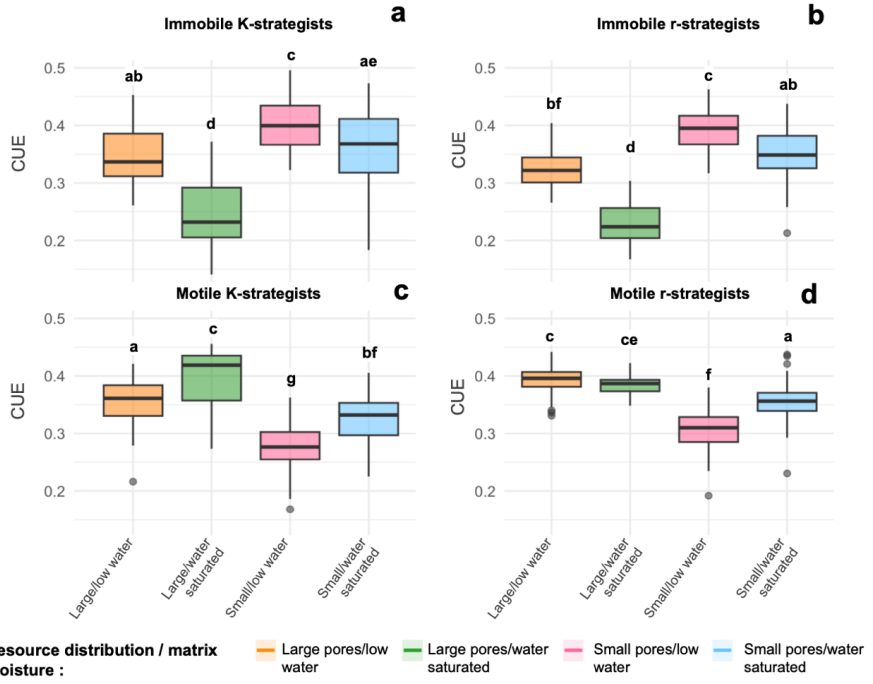

Figure 5 : Panel graph showing average CUE for each different cell type. Average CUE values were calculated from the 25th iteration onwards, in order to avoid the uncertainty associated with the population fluctuations at the beginning of the simulations. This analysis takes into account the 5 initial scenarios with r- and K-strategists separately for the two initial cell densities (28 and 56), as well as the mixed scenario with r- and K-strategists present together in the simulations. The colours used refer to the different initial matrix configurations. In orange and green, resources are distributed in the large pores, and in pink and blue, resources are distributed in the small pores. Green and blue refer to matrices saturated with water, and pink and orange to matrices with a one-pixel water film covering the solid phase of the soil and the resources. Letters on the figure refer to statistical differences between groups (Tuckey).

The motile cells with the largest CUE were observed in the large pores (Fig.5). In the case of motile K-strategists, these are large, water-saturated pores (CUE = 0.49±0.05), while in the case of motile r-strategists,

https://doi.org/10.5194/egusphere-2026-1818
Preprint. Discussion started: 10 April 2026

large pores, whether water-saturated or not, are indifferently associated with the highest CUE (Tukey: P=0.50). Also in contrast to what was described for immobile cells, small pores are the most constraining for the CUE of motile cells, with the lowest CUE particularly in small pores with low water content (CUE = 0.28±0.04 for K-strategists and CUE = 0.31±0.04 for r cells).

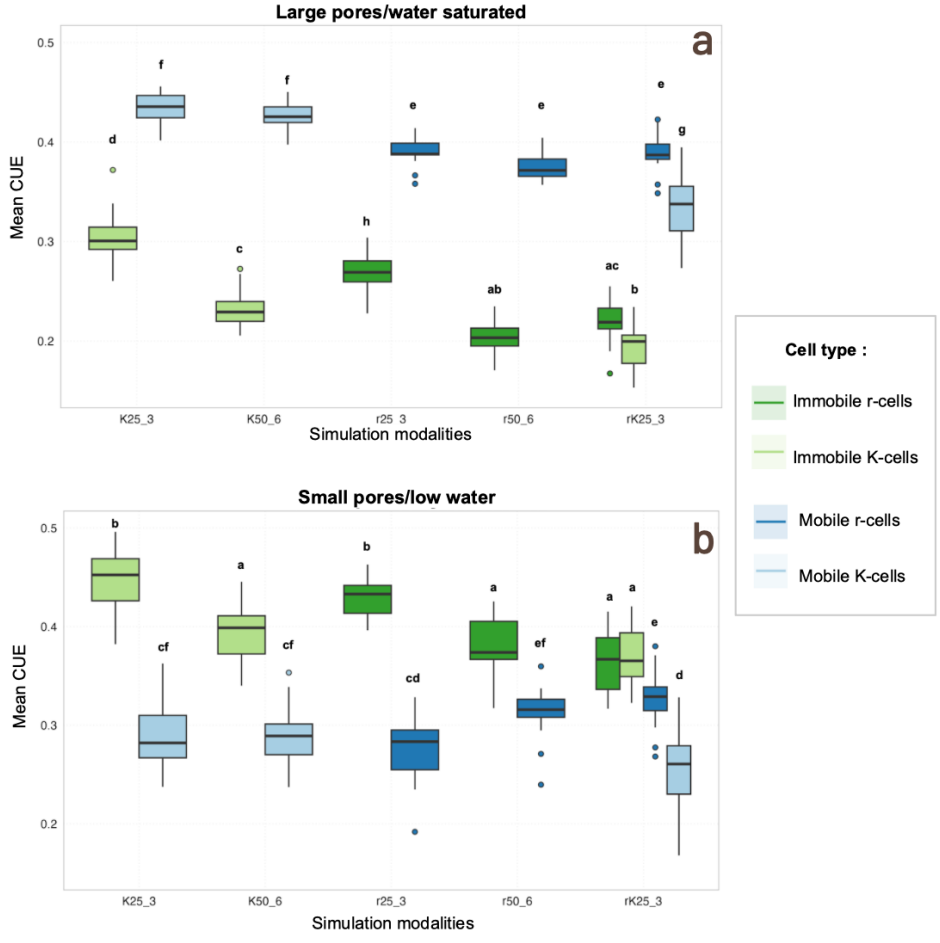

Figure 6 : Graphical panel showing the mean CUE in all the different initial matrix configurations, resources distributed in large pores or small pores with or without water saturation. Colours refer to the different cell types present in the matrices. K25_3 and K50_6 correspond to situations with K strategists only (25 immobile K cells and 3 motile K cells or 50 motile K cells and 6 immobile K cells respectively). r25_3 and r50_6 correspond to situations with r strategists only (25 immobile r cells and 3 motile r cells or 50 motile r cells and 6 immobile r cells respectively). rK25_3 show the results of simulations with competition, where r and K cells have been added jointly to the matrices (25 immobile K cells and 3 motile K cells with 25 motile r cells and 3 immobile r cells). The letters correspond to the statistical groups given by a Tuckey analysis, for each panel graph, the groups have been calculated separately.

The simulations with both r and K strategists enabled us to determine the effect of competition between the different cell types on CUE. Increasing the initial cell density significantly reduced CUE, the strategy of the cells

https://doi.org/10.5194/egusphere-2026-1818
Preprint. Discussion started: 10 April 2026

also had a significant effect, with K-strategists having higher CUE values. The K-strategist cells were more sensitive to the presence of r-strategists. In contrast, the CUE of r-strategists was less sensitive to the presence of K-strategists in the matrices. This competitive effect is largely modulated by the initial conditions of the matrices, the size of the resource distribution pores, but also humidity (Fig.6).

The results show that the initial configurations of the matrix had different effects on the cells; the two most distinct configurations were one in which the pore network was saturated with water, with resources distributed only in the large pores (Fig. 6b), and one in which water was limited and resources were found only in the small pores. When the pore network was water-saturated and resources were only in large pores (Fig. 6b), motile cells r were not affected by increasing cell density in the initial state (Tukey: P=0.32), nor by competition with motile cells K in the mixed situation (Tukey: P=0.99). However, this was not the case for motile K-strategists, whose CUE was negatively affected when there were motile r-strategists in the matrix (Tukey: P<0.001). In the case of immobile cells, r-strategists were affected at greater initial cell densities (Tukey: P< 0.001), regardless of whether these were r- or K-strategists (Tukey: P=0.36). The CUE of immobile K-strategists was reduced when the initial number of K-strategists was high (Tukey: P<0.001), and reduced further when in the presence of r-strategists (Tukey: P<0.001).

When resource was in small pores in low water conditions (Fig. 6c), the CUE of r-strategists was unaffected by the increase in initial cell density (Tukey HSD: P=0.001), and did not differ from the CUE of K-strategists (Tukey: P=0.98). The effects were different for motile K-strategists, whose CUE was not affected by high initial densities of K-strategists (Tukey: P=0.99), but were affected when in the presence of motile r-cells (Tukey: P<0.001). As far as immobile cells are concerned, the effects were identical for both cell strategies, with the CUE lowered by higher initial cell densities, regardless of their identity.

Discussion

4.1 Accuracy of the collected data

The population dynamics observed for motile cells, which were characterized by rapid growth following resource inputs, high turnover, and strong temporal fluctuations are consistent with rhizosphere population dynamics described in the literature (Darrah, 1991; Newman and Watson, 1977). We observed that microbial growth was limited by the supply of organic substrate, so an increase in microbial cell populations is associated with greater consumption of available resources in the environment, led to resource limitation and subsequently to the collapse of microbial populations. In the case of immobile cells, the population dynamics observed were more dependent on competition with motile cells for resources.

Although all cells are assumed to be the same size (1 pixel = 1 µm), they differ in their ability to accumulate resources, with K-strategists having higher reproduction thresholds. Consequently, these cells incur higher overall costs related to maintenance, motility and reproduction. To study the impact of these trade-offs, we ran supplementary simulations in which these costs were assigned arbitrarily so that we could observe the effect of simple variations allowing us to assess how differences in resource allocation influence microbial dynamics in a porous

https://doi.org/10.5194/egusphere-2026-1818
Preprint. Discussion started: 10 April 2026

space (Fig. S4). This modeling approach is consistent with theoretical predictions that the various costs associated with cellular life (motility, maintenance, reproduction) are closely linked to cell size (Kempes et al., 2017). In particular, motility depends heavily on cell size, and below a critical volume, directed motility is assumed to be inefficient and therefore absent (Dusenbery, 1997). When occuring in small microorganisms, motility can represent an energy cost comparable to, or even greater than, maintenance costs (Kempes et al., 2017).

Although few studies explicitly quantify the allocation of resources among these different expenditures, our parameterization yields microbial carbon use efficiency (CUE) values ranging from 0.28 to 0.78, which corresponds to values reported in the literature (He et al., 2024; Jones et al., 2018; Schnecker et al., 2023). Note that the CUE values reported for oligotrophic communities (up to 0.72; Ma et al., 2023) exceed our estimates, which probably reflects the simplifications inherent to our approach.

4.2 Influence of pore size and connectivity on microbial access to and microbial utilization of carbon

The model results suggest that the CUE of microorganisms is largely determined by the pore environment. It has already been shown that organic matter turnover varies across different soil pore sizes (Chenu et al., 2025; Li et al., 2024; Maestrali et al., 2026; Pfeiffer et al., 2001; Xia et al., 2022) because the microbes that dominate in these different pore sizes have strategies that are adapted to their microenvironment such as fluctuations in humidity (Ceriotti et al., 2022; Kravchenko et al., 2020), available space (Chenu et al., 2001; Gupta and Germida, 1988), nutrient availability (Bouckaert et al., 2013) and predation pressure (Erktan et al., 2020; Wright et al., 1995). This study suggests that the geometry of the pores themselves selects the microbes capable of colonising the environment. Indeed, when confined in micropores, organic matter is physically protected not only through exclusion by pore size, but also due to pore tortuosity, which modulates both substrate diffusion and microbial access. In our simulations, we observed that even when motile cells were close to small pores, their effective access to resources was limited by the tortuosity of the pore network. Although motile bacteria are capable of detecting chemical gradients, the establishment and continuity of these gradients depend on the connectivity of the pores and the continuity of the water film. In highly tortuous or poorly connected pore networks, chemical gradients can be weak, discontinuous, or spatially misleading, limiting the ability of motile cells to effectively reach nearby resource areas. For example, a flagellated bacterium may not effectively reach an organic matter particle located just a few micro-meters away if the accessible pathways are long or disconnected, whereas a non-motile bacterium already positioned nearby can exploit the resource via diffusion without incurring the energy cost of motility. These results are consistent with previous studies showing that tortuosity significantly influences bacterial mobility by increasing the complexity of the paths that bacteria must follow in porous media, thereby reducing their effective diffusion and transport rates. Using magnetic resonance imaging, it has been shown that the swimming behavior of bacteria such as *Pseudomonas putida* is strongly impeded by the pore structure (Olson et al., 2005). Bacterial motility patterns, particularly path lengths and turning angles, interact with surface adhesion in porous media, further increasing apparent tortuosity and affecting bacterial movement (Narayanaswamy et al., 2009). Experimental and modeling studies demonstrate that smaller pores and more tortuous paths reduce the average free-swimming distances of bacteria, hindering their self-propulsion (Dehkharghani et al., 2023; Duffy et al., 1995).

This mechanistic framework demonstrates that physical constraints at the pore scale alone can shape microbial activity and carbon use efficiency, independent of microbial size variation.

https://doi.org/10.5194/egusphere-2026-1818
Preprint. Discussion started: 10 April 2026

This work reveals the water regime (low water or water-saturated) modulates the influence of pore size on microbial communities. Under conditions with low water and organic matter in the macropores, motile cells achieve a higher CUE, suggesting that water creates connected pathways without completely restricting motility. This configuration allows motile cells to access resources while experiencing fewer diffusional constraints: resources diffuse only in the available water film and are therefore less 'diluted' compared to a situation where pores are completely saturated with water. Our simulations suggest that r-strategist populations, characterized by their rapid growth, exploit this situation particularly well by efficiently colonizing accessible surfaces.

4.3 Microbial motility as a competitive advantage depending on/across soil pore architecture

The simulations suggest that motility does not universally confer a competitive advantage, but instead leads to contrasting outcomes depending on pore-scale environmental conditions. In well-connected, carbon-rich environments, motile cells benefit from increased access to spatially distributed resources, resulting in higher growth and competitive success. In contrast, in poorly connected or resource-limited environments, the energetic costs associated with motility reduce carbon allocation to growth, leading to lower CUE compared to immobile strategies. This trade-off reflects the additional biosynthesis, repair, and operating costs associated with flagellar motility (Kempes et al., 2017), and is consistent with experimental observations showing reduced growth under carbon limitation when motility is constitutively expressed (Lisevich et al., 2025). Here, we show that pore-scale physical constraints modulate this trade-off, determining when motility enhances or limits microbial efficiency.

The architecture of pore networks fundamentally alters microbial movement and the advantage of motility. In fully saturated macropores, bacteria can exhibit efficient 'run-and-tumble' movements with long ballistic trajectories (Zhang et al., 2024). In contrast, in micropores, physical confinement forces motile cells to adopt a less efficient 'swim-and-stop' or 'jump-and-trap' movement, significantly eroding the advantages of motility. The chemotaxis machinery further amplifies these resource costs (for substrate detection, cilia or flagella movements, etc.), reducing the net CUE (van Albada et al., 2009; Hoffmann et al., 2017). In this context, the relationship between motility and carbon distribution is crucial. As this study demonstrates, motile bacteria have maximum CUE when organic matter is located in macropores, where chemotactic movement towards carbon gradients is optimal. When organic matter is confined to micropores, the motility advantage decreases significantly because bacteria cannot physically access these areas. In direct contrast, in our simulations, sessile bacteria dominate in micropores, maximising CUE by minimising motility-related costs (13–19% of the cellular resource budget in our models) and redirecting resources towards stress tolerance and growth efficiency. Indeed, in low-connectivity environments, Jin and Sengupta, (2024) observe that passive dispersal (expansion through growth, attachment to motile vectors) can surpass active motility in resource efficiency, explaining the good performance of immobile microbes when organic matter is confined to micropores. Thus, since the prevalence of bacterial flagellar motility is strongly associated with soil carbon accessibility (Ramoneda et al., 2024), cell motility should be particularly associated with a copiotrophic lifestyle, which explains the large populations observed in the case of motile r-strategists with resource distribution in the largest pores. Ultimately, the environmental dependencies observed (pore size, moisture) suggest that microbial communities are evolving towards motility patterns optimised for their specific environments. Microbial motility is not universally advantageous, but rather

https://doi.org/10.5194/egusphere-2026-1818
Preprint. Discussion started: 10 April 2026

represents a finely tuned adaptation to the interaction between pore architecture, carbon heterogeneity and resource trade-offs, with cascading effects on the carbon cycle at the ecosystem scale. Furthermore, under favourable moisture conditions, active cell motility plays a key role in the early colonisation process: Bacterial communities with cellular motility are pioneers and often the first to colonise new surfaces, followed by other bacteria with other functional traits (Wang et al., 2025), leading to the colonisation of new microenvironments in the soil.

4.4 Influence of pore size on the selection of microbial strategies (r or K)

The simulations show that pore architecture fundamentally structures microbial ecological strategies. It is known that micropores constitute preferential niches for oligotrophic taxa (Acidobacteriales, Frankiales, Firmicutes) specialised in the processing of complex carbon compounds (Li et al., 2024). These organisms have specific morphological adaptations, reduced cell sizes and filamentous shapes, that maximise nutrient absorption under resource-limited conditions (Chen et al., 2022).

Our simulations indicate that the environment, and in particular pore architecture, can strongly modulate the influence of life cycle parameters on carbon use efficiency (CUE). While r and K strategies represent well-established ecological archetypes (Pianka, 1970; Li et al., 2024), the conditions under which they maximise CUE are not universal but depend heavily on pore size and cell motility. Using a spatially-explicit model, our study shows that in large pores, maintenance cost emerged as the dominant parameter, influencing CUE outcomes differently for motile and immobile cells (Fig. 5). In small pores, the reproduction threshold played a central role. These results indicate that the effect of each parameters cannot be dissociated from the environmental context: the same parameter can improve CUE under certain pore conditions while limiting it under others (such as reproduction threshold). Similar results have been reported in microbial ecology, where the spatial heterogeneity of soil pores is recognised as a determining factor in microbial metabolic strategies (Nunan et al., 2020; Portell et al., 2018).

Carbon distribution in the soil pores network appears to be the main mechanistic link between pore size and the selection of microbial strategies. Chen et al., (2022) showed that carbon-rich rhizospheric soils favour copiotrophs, while poor environments select oligotrophs, which accentuates contrasts in resource availability between microsites. The microarchitecture of pores induces marked biogeochemical gradients over a few micrometres: Li et al., (2024) measured significant variations in oxygen, water film thickness and diffusion between pore classes, with macropores exhibiting more dynamic physicochemical conditions, while micropores maintain more stable but resource-poor environments. This trade-off between stability and availability is a fundamental axis for sorting ecological strategies, with r-strategists exploiting large, variable but rich pores, and K-strategists specialising in small, stable but limited pores. These spatio-temporal dynamics are also consistent with the phenomenon described by Zelenev et al., (2000) in the BACWAVE model, which simulated ‘bacterial waves’ generated by the movement of a nutrient pulse and translated into spatial waves of microbial growth and mortality along roots. Similarly, our model highlights a similar phenomenon where motile cells, particularly r-strategists, move along resource gradients formed on pore walls, producing wave-like dynamics of colonisation and consumption comparable to those observed empirically in the rhizosphere.

https://doi.org/10.5194/egusphere-2026-1818
Preprint. Discussion started: 10 April 2026

Our cellular automaton succeeds in reproducing several well-documented mechanisms of soil microbial ecology, such as the trade-offs between r and K strategies, the contrasted dynamics between motile and immobile cells, and the strong selective role of pore architecture on CUE. This convergence between model outputs and empirical knowledge highlights the potential of minimalistic, mechanistic approaches to capture emergent ecosystem patterns without requiring a high degree of parametrization. By making explicit the links between cellular traits, spatial constraints and carbon cycling, our framework provides a transparent testbed for exploring hypotheses that are difficult to address empirically at the microscale. Beyond confirming the relevance of r and K archetypes, our results pave the way for extending the model towards a broader trait-based framework, such as the Y-A-S triangle (Fig. S15) (Ho et al., 2013; Malik et al., 2020), in order to represent the continuum of microbial strategies observed in soils. This perspective opens promising avenues for coupling simple agent-based approaches with empirical measurements, ultimately contributing to a better mechanistic understanding of how microbial diversity and soil structure jointly shape the fate of carbon in terrestrial ecosystems.

Conclusion

This study employed a spatially explicit model to investigate how soil pore architecture, resource distribution, moisture and the life cycle characteristics of microorganisms jointly regulate microbial dynamics and carbon use efficiency. The results suggest that the physical structure is an active factor in microbial functioning, influencing both resource access and the outcome of ecological trade-offs.

Our results highlight that pore size and connectivity exert a dominant control over microbial carbon use efficiency (CUE), often surpassing the influence of intrinsic physiological parameters. In particular, heterogeneity at the pore scale determines whether traits such as motility confer a competitive advantage or become energetically detrimental. Motility emerges as a context-dependent strategy, beneficial in well-connected, resource-rich environments but disadvantageous under high spatial constraints or limited resource accessibility. Similarly, the performance of r- and K-strategies is not fixed but dynamically modulated by the spatial distribution of carbon and the physical accessibility imposed by pore networks. Beyond confirming established ecological patterns, our model reveals that microbial functioning cannot be understood without explicitly accounting for the interaction between spatial structure and trait trade-offs.

Our model supports the use of minimalist yet mechanistic approaches as powerful tools for bridging the gap between pore-scale processes and the ecosystem-scale carbon cycle. However, several limitations must be acknowledged. The assumption of complete and instantaneous recycling of microbial biomass, as well as the simplified representation of microbial traits, likely leads to an overestimation of carbon turnover rates. Future developments should aim to incorporate more realistic representations of necromass dynamics, the effect of mineral surfaces, and a broader continuum of microbial strategies. By explicitly linking pore geometry and microbial ecology, this work offers a new conceptual framework for improving our understanding of the carbon cycle at the fine scale.

Code availability

https://doi.org/10.5194/egusphere-2026-1818
Preprint. Discussion started: 10 April 2026

Data availability

The Python and R code used to run the cellular automaton is available on request. The data and the R code used for statistical analysis are also available on request.

Author contributions

MM: Conceptualisation, data curation, formal analysis, methodology, visualisation, writing ; XR: Conceptualisation, methodology, validation, writing (review and editing); NN: Writing (review and editing), validation, supervision; HW: Conceptualisation, validation ; NN: Writing (review and editing), validation, supervision; ASR : data curation, formal analysis, visualisation.

Competing interests

The authors have no competing interests to declare.

Special issue statement

This article is part of the special issue “Advances in dynamic soil modelling across scales”. It is not associated with a conference.

Acknowledgements

This research was supported by the Deutsche Forschungsgemeinschaft (DFG) and the Agence Nationale de la Recherche (ANR) as part of the SoilPACMAN Project (DFG project no. 505667051). We gratefully acknowledge their funding and support.

Financial support

This research was directly funded by and the Agence Nationale de la Recherche (ANR), ANR-22-CE92-0039-01.

https://doi.org/10.5194/egusphere-2026-1818
Preprint. Discussion started: 10 April 2026

592 A Malik, A., Martiny, J. B. H., Brodie, E. L., Martiny, A. C., Treseder, K. K., and Allison, S. D.: Defining trait-
593 based microbial strategies with consequences for soil carbon cycling under climate change | The ISME Journal |
594 Oxford Academic, The ISME Journal, 14, Pages 1-9, 2020.

595 van Albada, S. B., Tănase-Nicola, S., and ten Wolde, P. R.: The switching dynamics of the bacterial flagellar
596 motor, Molecular Systems Biology, 5, 316, https://doi.org/10.1038/msb.2009.74, 2009.

597 Allison, S. D.: Cheaters, diffusion and nutrients constrain decomposition by microbial enzymes in spatially
598 structured environments, Ecology Letters, 8, 626–635, https://doi.org/10.1111/j.1461-0248.2005.00756.x, 2005.

599 Barton: Mathematical model for characterization of bacterial migration through sand cores, Biotechnology and
600 Bioengineering, 1997.

601 Baveye, P. C., Rangel, D., Jacobson, A. R., Laba, M., Darnault, C., Otten, W., Radulovich, R., and Camargo, F.
602 A. O.: From Dust Bowl to Dust Bowl: Soils are Still Very Much a Frontier of Science, Soil Science Society of
603 America Journal, 75, 2037–2048, https://doi.org/10.2136/sssaj2011.0145, 2011.

604 Bongiorno, G., Bünemann, E. K., Oguejiofor, C. U., Meier, J., Gort, G., Comans, R., Mäder, P., Brussaard, L.,
605 and de Goede, R.: Sensitivity of labile carbon fractions to tillage and organic matter management and their po-
606 tential as comprehensive soil quality indicators across pedoclimatic conditions in Europe, Ecological Indicators,
607 99, 38–50, https://doi.org/10.1016/j.ecolind.2018.12.008, 2019.

608 Bouckaert, L., Sleutel, S., Loo, D. V., Brabant, L., Cnudde, V., Hoorebeke, L. V., and Neve, S. D.: Carbon mine-
609 ralisation and pore size classes in undisturbed soil cores, Soil Res., 51, 14–22, https://doi.org/10.1071/SR12116,
610 2013.

611 Bresenham, J. E.: Algorithm for computer control of a digital plotter, IBM Systems Journal, 4, 25–30,
612 https://doi.org/10.1147/sj.41.0025, 1965.

613 Ceriotti, G., Borisov, M., S, S. B., J, D. A., and P.: Morphology and Size of Bacterial Colonies Control Anoxic
614 Microenvironment Formation in Porous Media, , https://doi.org/10.1021/acs.est.2c05842, 2022.

615 Chang, W.-S., Li, X., and Halverson, L. J.: Influence of water limitation on endogenous oxidative stress and cell
616 death within unsaturated Pseudomonas putida biofilms, Environ Microbiol, 11, 1482–1492,
617 https://doi.org/10.1111/j.1462-2920.2009.01876.x, 2009.

618 Chen, H., Jing, Q., Liu, X., Zhou, X., Fang, C., Li, B., Zhou, S., and Nie, M.: Microbial respiratory thermal
619 adaptation is regulated by r-/K-strategy dominance, Ecol Lett, 25, 2489–2499, https://doi.org/10.1111/ele.14106,
620 2022.

621 Chenu, C., Hassink, J., and Bloem, J.: Short-term changes in the spatial distribution of microorganisms in soil
622 aggregates as affected by glucose addition, Biol Fertil Soils, 34, 349–356,
623 https://doi.org/10.1007/s003740100419, 2001.

624 Chenu, C., Pouteau, V., and Nunan, N.: Pore scale microbial biogeography across different soil types, Soil Bio-
625 logy and Biochemistry, 209, 109896, https://doi.org/10.1016/j.soilbio.2025.109896, 2025.

626 Chunhua Lv: Rhizosphere effects on soil organic carbon processes in terrestrial ecosystems: A meta-analysis,
627 Geoderma, 412, 115739, https://doi.org/10.1016/j.geoderma.2022.115739, 2022.

628 Darrah, P. R.: Models of the rhizosphere: I. Microbial population dynamics around a root releasing soluble and
629 insoluble carbon, Plant Soil, 133, 187–199, https://doi.org/10.1007/BF00009191, 1991.

630 Dehkharghani, A., Waisbord, N., and Guasto, J. S.: Self-transport of swimming bacteria is impaired by porous
631 microstructure, Commun Phys, 6, 18, https://doi.org/10.1038/s42005-023-01136-w, 2023.

632 Dignac, M.-F., Derrien, D., Barré, P., Barot, S., Cécillon, L., Chenu, C., Chevallier, T., Freschet, G. T., Garnier,
633 P., Guenet, B., Hedde, M., Klumpp, K., Lashermes, G., Maron, P.-A., Nunan, N., Roumet, C., and Basile-
634 Doelsch, I.: Increasing soil carbon storage: mechanisms, effects of agricultural practices and proxies. A review,
635 Agron. Sustain. Dev., 37, 14, https://doi.org/10.1007/s13593-017-0421-2, 2017.

https://doi.org/10.5194/egusphere-2026-1818
Preprint. Discussion started: 10 April 2026

636 Duffy, K. J., Cummings, P. T., and Ford, R. M.: Random walk calculations for bacterial migration in porous me-
637 dia, Biophysical Journal, 68, 800–806, https://doi.org/10.1016/S0006-3495(95)80256-0, 1995.

638 Dusenbery, D. B.: Minimum size limit for useful locomotion by free-swimming microbes, Proceedings of the
639 National Academy of Sciences, 94, 10949–10954, https://doi.org/10.1073/pnas.94.20.10949, 1997.

640 Erktan, A., Or, D., and Scheu, S.: The physical structure of soil: Determinant and consequence of trophic interac-
641 tions, Soil Biology and Biochemistry, 148, 107876, https://doi.org/10.1016/j.soilbio.2020.107876, 2020.

642 Fierer, N., Bradford, M. A., and Jackson, R. B.: Toward an Ecological Classification of Soil Bacteria, Ecology,
643 88, 1354–1364, https://doi.org/10.1890/05-1839, 2007.

644 Franzluebbers, A. J., Hons, F. M., and Zuberer, D. A.: Seasonal changes in soil microbial biomass and mineral-
645 izable c and n in wheat management systems, Soil Biology and Biochemistry, 26, 1469–1475,
646 https://doi.org/10.1016/0038-0717(94)90086-8, 1994.

647 Gao, Y., Zhou, J., Lin, T., Li, Y., Zeng, Q., Chen, S., Xiong, D., Zhang, Q., Yang, Z., and Yang, Y.: The domi-
648 nance of K-strategy microbes enhances the potential of soil carbon decomposition under long-term warming,
649 Applied Soil Ecology, 206, 105854, https://doi.org/10.1016/j.apsoil.2024.105854, 2025.

650 Gupta, V. V. S. R. and Germida, J. J.: Distribution of microbial biomass and its activity in different soil aggre-
651 gate size classes as affected by cultivation, Soil Biology and Biochemistry, 20, 777–786,
652 https://doi.org/10.1016/0038-0717(88)90082-X, 1988.

653 Haynes, R. J.: Labile Organic Matter Fractions as Central Components of the Quality of Agricultural Soils: An
654 Overview, 85, 221–268, https://doi.org/10.1016/S0065-2113(04)85005-3, 2005.

655 He, L., Lipson, D. A., Mazza Rodrigues, J. L., Mayes, M., Björk, R. G., Glaser, B., Thornton, P., and Xu, X.:
656 Dynamics of Fungal and Bacterial Biomass Carbon in Natural Ecosystems: Site-Level Applications of the CLM-
657 Microbe Model, Journal of Advances in Modeling Earth Systems, 13, e2020MS002283,
658 https://doi.org/10.1029/2020MS002283, 2021.

659 He, X., Abs, E., Allison, S. D., Tao, F., Huang, Y., Manzoni, S., Abramoff, R., Bruni, E., Bowring, S. P. K.,
660 Chakrawal, A., Ciais, P., Elsgaard, L., Friedlingstein, P., Georgiou, K., Hugelius, G., Holm, L. B., Li, W., Luo,
661 Y., Marmasse, G., Nunan, N., Qiu, C., Sitch, S., Wang, Y.-P., and Goll, D. S.: Emerging multiscale insights on
662 microbial carbon use efficiency in the land carbon cycle, Nature Communications, 15, 8010,
663 https://doi.org/10.1038/s41467-024-52160-5, 2024.

664 Ho, A., Kerckhof, F.-M., Luke, C., Reim, A., Krause, S., Boon, N., and Bodelier, P. L. E.: Conceptualizing func-
665 tional traits and ecological characteristics of methane-oxidizing bacteria as life strategies, Environmental Micro-
666 biology Reports, 5, 335–345, https://doi.org/10.1111/j.1758-2229.2012.00370.x, 2013.

667 Hoffmann, S., Schmidt, C., Walter, S., Bender, J. K., and Gerlach, R. G.: Scarless deletion of up to seven
668 methyl-accepting chemotaxis genes with an optimized method highlights key function of CheM in Salmonella
669 Typhimurium, PLOS ONE, 12, e0172630, https://doi.org/10.1371/journal.pone.0172630, 2017.

670 Jenkinson, D. S. and Powlson, D. S.: The effects of biocidal treatments on metabolism in soil—V: A method for
671 measuring soil biomass, Soil Biology and Biochemistry, 8, 209–213, https://doi.org/10.1016/0038-
672 0717(76)90005-5, 1976.

673 Jin, C. and Sengupta, A.: Microbes in porous environments: from active interactions to emergent feedback, Bio-
674 phys Rev, https://doi.org/10.1007/s12551-024-01185-7, 2024.

675 Jones, D. L., Hill, P. W., Smith, A. R., Farrell, M., Ge, T., Banning, N. C., and Murphy, D. V.: Role of substrate
676 supply on microbial carbon use efficiency and its role in interpreting soil microbial community-level physiologi-
677 cal profiles (CLPP), Soil Biology and Biochemistry, 123, 1–6, https://doi.org/10.1016/j.soilbio.2018.04.014,
678 2018.

679 Kästner, M., Miltner, A., Thiele-Bruhn, S., and Liang, C.: Microbial Necromass in Soils—Linking Microbes to
680 Soil Processes and Carbon Turnover, Front. Environ. Sci., 9, https://doi.org/10.3389/fenvs.2021.756378, 2021.

https://doi.org/10.5194/egusphere-2026-1818
Preprint. Discussion started: 10 April 2026

Kempes, C. P., van Bodegom, P. M., Wolpert, D., Libby, E., Amend, J., and Hoehler, T.: Drivers of Bacterial Maintenance and Minimal Energy Requirements, Front. Microbiol., 8, https://doi.org/10.3389/fmicb.2017.00031, 2017.

Killham, K., Amato, M., and Ladd, J. N.: Effect of substrate location in soil and soil pore-water regime on carbon turnover, Soil Biology and Biochemistry, 25, 57–62, 1993.

Kravchenko, A. N. and Guber, A. K.: Soil pores and their contributions to soil carbon processes, Geoderma, 287, 31–39, https://doi.org/10.1016/j.geoderma.2016.06.027, 2017.

Kravchenko, A. N., Guber, A. K., Razavi, B. S., Koestel, J., Quigley, M. Y., Robertson, G. P., and Kuzyakov, Y.: Reply to: "Variables in the effect of land use on soil extrapore enzymatic activity and carbon stabilization" by Glenn (2020, Nat Commun, 11, 6427, 2020.

Lehmann, J., Hansel, C., Kaiser, C., Kleber, M., Maher, K., Manzoni, S., Nunan, N., Reichstein, M., Schimel, J., and Torn, M.: Persistence of soil organic carbon caused by functional complexity, Nature Geoscience, 13, 1–6, 2020.

Li, Z., Kravchenko, A. N., Cupples, A., Guber, A. K., Kuzyakov, Y., Philip Robertson, G., and Blagodatskaya, E.: Composition and metabolism of microbial communities in soil pores, Nat Commun, 15, 3578, https://doi.org/10.1038/s41467-024-47755-x, 2024.

Liang, C., Amelung, W., Lehmann, J., and Kästner, M.: Quantitative assessment of microbial necromass contribution to soil organic matter, Global Change Biology, 25, 3578–3590, https://doi.org/10.1111/gcb.14781, 2019.

Lisevich, I., Colin, R., Yang, H. Y., Ni, B., and Sourjik, V.: Physics of swimming and its fitness cost determine strategies of bacterial investment in flagellar motility, Nat Commun, 16, 1731, https://doi.org/10.1038/s41467-025-56980-x, 2025.

Ma, S., Zhu, W., Wang, W., Li, X., and Sheng, Z.: Microbial assemblies with distinct trophic strategies drive changes in soil microbial carbon use efficiency along vegetation primary succession in a glacier retreat area of the southeastern Tibetan Plateau, Sci Total Environ, 867, 161587, https://doi.org/10.1016/j.scitotenv.2023.161587, 2023.

Maestrali, M., Raynaud, X., Wu, H., Schweizer, S. A., Guillot, I., Lerch, T., Paolillo, S., and Nunan, N.: How is the carbon use efficiency of microbial communities distributed within the soil pore network, Applied Soil Ecology, 219, 106771, https://doi.org/10.1016/j.apsoil.2025.106771, 2026.

McLauchlan, K. K. and Hobbie, S. E.: Comparison of Labile Soil Organic Matter Fractionation Techniques, Soil Science Society of America Journal, 68, 1616–1625, https://doi.org/10.2136/sssaj2004.1616, 2004.

Narayanaswamy, K., Ford, R. M., Smith, J. A., and Fernandez, E. J.: Surface association of motile bacteria and apparent tortuosity values in packed column experiments, Water Resources Research, 45, https://doi.org/10.1029/2008WR006851, 2009.

Newman, E. I. and Watson, A.: Microbial abundance in the rhizosphere: A computer model, Plant Soil, 48, 17–56, https://doi.org/10.1007/BF00015157, 1977.

Olson, M. S., Ford, R. M., Smith, J. A., and Fernandez, E. J.: Analysis of Column Tortuosity for MnCl2 and Bacterial Diffusion Using Magnetic Resonance Imaging, Environ. Sci. Technol., 39, 149–154, https://doi.org/10.1021/es049577x, 2005.

Or, D., Smets, B. F., Wraith, J. M., Dechesne, A., and Friedman, S. P.: Physical constraints affecting bacterial habitats and activity in unsaturated porous media – a review, Advances in Water Resources, 30, 1505–1527, https://doi.org/10.1016/j.advwatres.2006.05.025, 2007.

Otten, W., Hall, D., Harris, K., Ritz, K., Young, I. M., and Gilligan, C. A.: Soil physics, fungal epidemiology and the spread of Rhizoctonia solani, New Phytologist, 151, 459–468, https://doi.org/10.1046/j.0028-646x.2001.00190.x, 2001.

https://doi.org/10.5194/egusphere-2026-1818
Preprint. Discussion started: 10 April 2026

Panikov, N. S.: Understanding and prediction of soil microbial community dynamics under global change, Applied Soil Ecology, 11, 161–176, https://doi.org/10.1016/S0929-1393(98)00143-7, 1999.

Peng, J., Liu, H., Sun, Y., Liu, Q., Li, J., and Dong, Y.: Shift in soil bacterial communities from K- to r-strategists facilitates adaptation to grassland degradation, Land Degradation & development, 33, https://doi.org/https://doi.org/10.1002/ldr.4304, 2022.

Pfeiffer, T., Schuster, S., and Bonhoeffer, S.: Cooperation and Competition in the Evolution of ATP-Producing Pathways, Science, 292, 504–507, https://doi.org/10.1126/science.1058079, 2001.

Pot, V., Portell, X., Otten, W., Garnier, P., Monga, O., and Baveye, P. C.: Accounting for soil architecture and microbial dynamics in microscale models: Current practices in soil science and the path ahead, European Journal of Soil Science, 2021.

R: The R Project for Statistical Computing: https://www.r-project.org/, last access: 11 February 2026.

Rabot, E., Wiesmeier, M., Schlüter, S., and Vogel, H.-J.: Soil structure as an indicator of soil functions: A review, Geoderma, 314, 122–137, 2018.

Ramoneda, J., Fan, K., Lucas, J. M., Chu, H., Bissett, A., Strickland, M. S., and Fierer, N.: Ecological relevance of flagellar motility in soil bacterial communities, The ISME Journal, 18, wrae067, https://doi.org/10.1093/ismejo/wrae067, 2024.

Ray, N., Rupp, A., and Prechtel, A.: Discrete-continuum multiscale model for transport, biomass development and solid restructuring in porous media, Advances in Water Resources, 107, 393–404, https://doi.org/10.1016/j.advwatres.2017.04.001, 2017.

Reznick, D., Bryant, M., and Bashey, F.: r- and K-Selection Revisited: The Role of Population Regulation in Life-History Evolution, Ecology, 83, 1509–1520, https://doi.org/10.2307/3071970, 2002.

Ritschel, T. and Totsche, K. U.: Modeling the formation of soil microaggregates, Computers & Geosciences, 127, 36–43, https://doi.org/10.1016/j.cageo.2019.02.010, 2019.

Rötzer, M., Braunmiller, H., Lehndorff, E., Ray, N., Scheibe, A., and Prechtel, A.: Coupled C and N turnover in a dynamic pore scale model reveal the impact of exudate quality on microbial necromass formation, https://doi.org/10.5194/egusphere-2025-4717, 14 October 2025.

Ruamps, L., Nunan, N., and Chenu, C.: Microbial biogeography at the soil pore scale, Soil Biology & Biochemistry, 43, 280–286, https://doi.org/10.1016/j.soilbio.2010.10.010, 2011.

Saltelli, A., Chan, K., and Scott, E. M.: Sensitivity Analysis: Gauging the Worth of Scientific Models, John Wiley & Sons, 515 pp., 2000.

Schimel, J. and Schaeffer, S. M.: Microbial control over carbon cycling in soil, Front. Microbiol., 3, https://doi.org/10.3389/fmicb.2012.00348, 2012.

Schlüter, S., Sammartino, S., and Koestel, J.: Exploring the relationship between soil structure and soil functions via pore-scale imaging, Geoderma, 370, 114370, https://doi.org/10.1016/j.geoderma.2020.114370, 2020.

Schlüter, S., Gil, E., Doniger, T., Applebaum, I., and Steinberger, Y.: Abundance and community composition of free-living nematodes as a function of soil structure under different vineyard managements, Applied Soil Ecology, 170, 104291, https://doi.org/10.1016/j.apsoil.2021.104291, 2022.

Schnecker, J., Baldaszti, L., Gündler, P., Pleitner, M., Sandén, T., Simon, E., Spiegel, F., Spiegel, H., Urbina Malo, C., Zechmeister-Boltenstern, S., and Richter, A.: Seasonal dynamics of soil microbial growth, respiration, biomass, and carbon use efficiency in temperate soils, Geoderma, 440, 116693, https://doi.org/10.1016/j.geoderma.2023.116693, 2023.

https://doi.org/10.5194/egusphere-2026-1818
Preprint. Discussion started: 10 April 2026

766 Shi, A., Chakrawal, A., Manzoni, S., Fischer, B. M. C., Nunan, N., and Herrmann, A. M.: Substrate spatial hete-
767 rogeneity reduces soil microbial activity, Soil Biology and Biochemistry, 152, 108068,
768 https://doi.org/10.1016/j.soilbio.2020.108068, 2021.

769 Smet, S., Plougonven, E., Leonard, A., Degré, A., and Beckers, E.: X-ray Micro-CT: How Soil Pore Space Des-
770 cription Can Be Altered by Image Processing, Vadose Zone Journal, 17, 160049,
771 https://doi.org/10.2136/vzj2016.06.0049, 2018.

772 Sparling, G. P. and West, A. W.: A direct extraction method to estimate soil microbial C: calibration *in situ* using
773 microbial respiration and 14C labelled cells, Soil Biology and Biochemistry, 20, 337–343,
774 https://doi.org/10.1016/0038-0717(88)90014-4, 1988.

775 Wang, G. and Or, D.: Aqueous films limit bacterial cell motility and colony expansion on partially saturated
776 rough surfaces, Environmental Microbiology, 12, 1363–1373, https://doi.org/10.1111/j.1462-2920.2010.02180.x,
777 2010.

778 Wang, Y., Ebrahimi, A., Chen, G., Zhang, Z., Zhu, K., Franklin, S., Jin, Y., Liu, Y., and Wang, G.: Active moti-
779 lity and chemotactic movement regulate the microbial early-colonization and biodiversity, Geoderma, 460,
780 117419, https://doi.org/10.1016/j.geoderma.2025.117419, 2025.

781 Wolfram, S.: A New Kind of Science, Wolfram Media Inc., 2002.

782 Wright, D. A., Killham, K., Glover, L. A., and Prosser, J. I.: Role of Pore Size Location in Determining Bacterial
783 Activity during Predation by Protozoa in Soil, Appl Environ Microbiol, 61, 3537–3543, 1995.

784 Xia, Q., Zheng, N., Heitman, J. L., and Shi, W.: Soil pore size distribution shaped not only compositions but also
785 networks of the soil microbial community, Applied Soil Ecology, 170, 104273,
786 https://doi.org/10.1016/j.apsoil.2021.104273, 2022.

787 Young, I. M. and Crawford, J. W.: Interactions and Self-Organization in the Soil-Microbe Complex, Science,
788 304, 1634–1637, https://doi.org/10.1126/science.1097394, 2004.

789 Zaitsev, D. A.: A generalized neighborhood for cellular automata, Theoretical Computer Science, 666, 21–35,
790 https://doi.org/10.1016/j.tcs.2016.11.002, 2017.

791 Zech, S., Ritschel, T., Ray, N., Totsche, K. U., and Prechtel, A.: How water connectivity and substrate supply
792 shape the turnover of organic matter – Insights from simulations at the scale of microaggregates, Geoderma, 405,
793 115394, https://doi.org/10.1016/j.geoderma.2021.115394, 2022.

794 Zelenev, V. V., van Bruggen, A. H. C., and Semenov, A. M.: "BACWAVE," a Spatial-Temporal Model for Tra-
795 veling Waves of Bacterial Populations in Response to a Moving Carbon Source in Soil, Microbial Ecology, 40,
796 260–272, 2000.

797 Zhang, H., Wetherington, M. T., Ko, H., FitzGerald, C. E., and Nirody, J. A.: Bacterial motility patterns adapt
798 smoothly in response to spatial confinement and disorder, https://doi.org/10.1101/2024.09.29.615714, 30 Sep-
799 tember 2024.

800 Zhao, X., Tian, P., Sun, Z., Liu, S., Wang, Q., and Zeng, Z.: Rhizosphere effects on soil organic carbon pro-
801 cesses in terrestrial ecosystems: A meta-analysis, Geoderma, 412, 115739,
802 https://doi.org/10.1016/j.geoderma.2022.115739, 2022.

803 Zheng, W., Fan, X., Chen, H., Ye, M., Yin, C., Wu, C., and Liang, Y.: The response patterns of r- and K-
804 strategist bacteria to long-term organic and inorganic fertilization regimes within the microbial food web are clo-
805 sely linked to rice production, Science of The Total Environment, 942, 173681,
806 https://doi.org/10.1016/j.scitotenv.2024.173681, 2024.

807